An improved memristor model for brain-inspired computing*

Errui Zhou(周二瑞), Liang Fang(方粮)†, Rulin Liu(刘汝霖), and Zhenseng Tang(汤振森)

State Key Laboratory of High Performance Computing, College of Computer, National University of Defense Technology, Changsha 410073, *China*

(Received 10 May 2017; revised manuscript received 17 August 2017; published online 30 September 2017)

Memristors, as memristive devices, have received a great deal of interest since being fabricated by HP labs. The forgetting effect that has significant influences on memristors' performance has to be taken into account when they are employed. It is significant to build a good model that can express the forgetting effect well for application researches due to its promising prospects in brain-inspired computing. Some models are proposed to represent the forgetting effect but do not work well. In this paper, we present a novel window function, which has good performance in a drift model. We analyze the deficiencies of the previous drift diffusion models for the forgetting effect and propose an improved model. Moreover, the improved model is exploited as a synapse model in spiking neural networks to recognize digit images. Simulation results show that the improved model overcomes the defects of the previous models and can be used as a synapse model in brain-inspired computing due to its synaptic characteristics. The results also indicate that the improved model can express the forgetting effect better when it is employed in spiking neural networks, which means that more appropriate evaluations can be obtained in applications.

Keywords: memristor, drift diffusion model, synaptic, brain-inspired computing

PACS: 85.35.–p, 87.19.lv, 87.19.lw **DOI:** 10.1088/1674-1056/26/11/118502

1. Introduction

The memristor, called the fourth fundamental element besides resistor, capacitor, and inductor, was predicted by Prof. Chua theoretically in 1971.[1] It has received broad attention since being discovered by HP labs in 2008.[2] The memristor has broad prospects in many fields: it is a promising candidate for nonvolatile memory and may change the existing computer structure,[3–5] and it can be employed in image processing and other fields.[6,7] What is more, it is a promising candidate for synaptic devices in brain-inspired computing.[8–10] In this context, it is significant to build a good model for memristor application research.

HP labs presented a drift model when they discovered the first memristor.[2] However, HP's model has some significant deficiencies; several window functions have been proposed to improve it. Joglekar *et al.* proposed a window function to overcome the terminal overflow; Biolek *et al.* proposed a window function to solve the terminal lock and so on.[11–14] However, these window functions have their blemishes more or less. In this paper, a novel window function is proposed. It can overcome the terminal overflow and terminal lock and has good flexibility.

In later studies, researchers found the forgetting effect in several experiments, which is also called short term memory or volatile memory.[15–17] In order to describe this phenomenon, many models have been proposed.[15,18,19] Berdan *et al.* and Ling Chen *et al.* proposed different drift diffusion models based on research results of Strukov.[20–22] Though both models can describe the forgetting effect to some extent, they have some deficiencies that the forgetting effect in terminal ($x = 0$, 1) cannot be embodied in some situation that is common in fact. The forgetting effect has essential influences on accuracies and functions of applications, such as non-volatile memory and brain-inspired computing based on memristors. When a memristor model that cannot express the forgetting effect well is employed in simulations, it may cause serious errors. In this paper, we present an improved drift diffusion model to overcome shortcomings of the previous models. The threshold characteristic is added to our model since the existence of threshold has been discovered in several memristors. Spike-timing-dependent plasticity (STDP) of our model is verified, which means that the improved model can be employed as a synapse model. Moreover, the improved model is used in spiking neural networks (SNNs) to prove its merits. Simulation results indicate that the improved model can overcome deficiencies of the previous works and it can express the forgetting effect better when it is used as the synapse model in SNNs.

2. Window function

2.1. Existing window functions

The drift model proposed by HP labs is shown in Fig. 1. It can be seen that there are two regions in a memristor: the doped region and the undoped region, and there is a boundary between them. D is the length of the memristor and w is the length of the doped region.

*Project supported by the National Natural Science Foundation of China (Grant No. 61332003) and High Performance Computing Laboratory, China (Grant No. 201501-02).

†Corresponding author. E-mail: lfang@nudt.edu.cn

© 2017 Chinese Physical Society and IOP Publishing Ltd

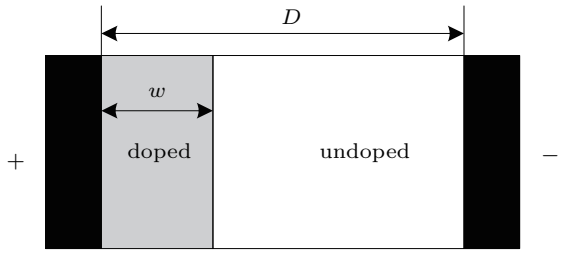


Fig. 1. HP's drift model.

The model is described as

$$R_{\rm mem}(x) = R_{\rm on}x + R_{\rm off}(1-x), \quad x = \frac{w}{D} \in (0,1), \tag{1}$$

$$v(t) = R_{\rm mem}(w)i(t), \tag{2}$$

$$\frac{{\rm d}x}{{\rm d}t} = \frac{\mu_{\rm v}R_{\rm on}}{D^2}i(t), \tag{3}$$

where $R_{\rm on}$ is the resistance when the memristor is completely doped, and $R_{\rm off}$ is the resistance when the memristor is undoped. $x = w/D$ is the ratio of the doped region, $v(t)$ is the voltage applied on the memristor, $i(t)$ is the current flowing through the memristor, and $\mu_{\rm v}$ is the mobility of oxygen vacancies. HP's model can describe characteristics of memristors to some extent, but it has many defects. A significant one is that x can overflow the scale of [0, 1] when there is a continuous positive (negative) stimulus on the memristor, also called the terminal overflow.

In order to improve HP's drift model, many window functions have been proposed. Jogleka's window function is expressed as

$$f(x) = 1 - (2x-1)^{2p}. \tag{4}$$

Then expression (3) is modified to

$$\frac{{\rm d}x}{{\rm d}t} = \frac{\mu_{\rm v}R_{\rm on}}{D^2}i(t)f(x). \tag{5}$$

This window function makes x not move when $x = 0$, 1, i.e., ${\rm d}x/{\rm d}t = 0$, so x cannot overflow the scale of [0, 1], as shown in Fig. 2(a). However, there is a problem that x can no longer move when $x = 0$, 1 even though there is a reversed stimulus, which is also called terminal lock. Biolek *et al.* proposed the following window function to solve the terminal lock:

$$f(x) = 1 - (x - {\rm stp}(-i))^{2p}, \tag{6}$$

$${\rm stp}(i) = \begin{cases} 1, & \text{if } i \geq 0, \\ 0, & \text{if } i < 0. \end{cases} \tag{7}$$

Biolek's window function takes the current direction into account, as shown in Fig. 2(b). When $i(t) > 0$, expression (6) turns into $f(x) = 1 - x^{2p}$, and $f(0) = 1$, $f(1) = 0$. When $i(t) \leq 0$, expression (6) turns into $f(x) = 1 - (x-1)^{2p}$, and $f(0) = 0$, $f(1) = 1$. Biolek's window function solves the terminal overflow and terminal lock. However, the parameter p must have positive integers, which limits the flexibility of the window function. Then Prodomakis *et al.* proposed a window function

$$f(x) = j(1 - ((x-0.5)^2 + 0.75)^p), \tag{8}$$

which has good flexibility and overcomes the terminal overflow, but cannot solve the terminal lock. Other window functions are being proposed continuously. However, their advantages are accompanied by disadvantages.

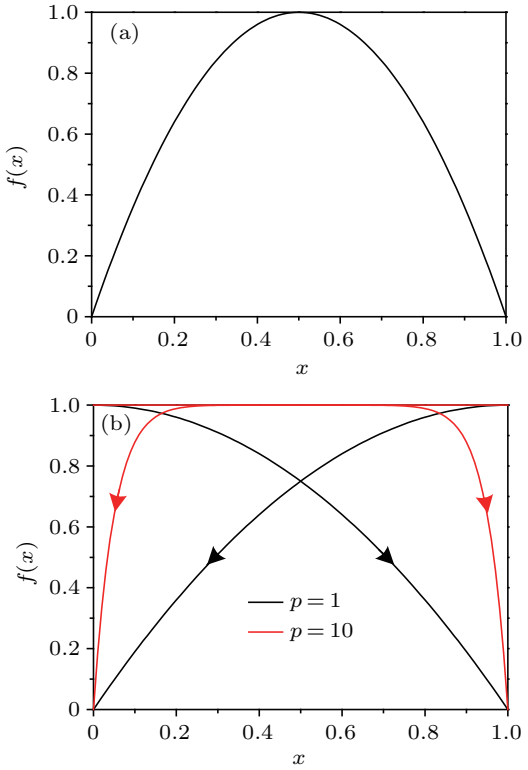


Fig. 2. (color online) (a) Jogleka's window function and (b) Biolek's window function.

2.2. Novel window function

It is easy to know that function $y = 1/x$ is a decreasing function in (0, $+\infty$). So it can be exploited as a basic model of the window function, and the model can be expressed as $f(x) = 1/(ax+b) + c$. When the stimulus is positive and x increases continuously, it is necessary to make $f(0) = 1$ and $f(1) = 0$. A set of solutions are $a = b = 1/2$ and $c = -1$, the function is $f_1(x) = 2/(x+1) - 1$. When the stimulus is negtive and x decreases continuously, it is easy to obtain $f_2(x) = 2/(2-x) - 1$. Then considering $f_1(x)$ and $f_2(x)$ comprehensively, we introduce

$$f(x) = \frac{2}{1.5 + {\rm sgn}(i)(x-0.5)} - 1,$$

$${\rm sgn}(i) = \begin{cases} 1, & i \geq 0. \\ -1, & i < 0. \end{cases} \tag{9}$$

In order to increase the flexibility of expression (9), exponent p and coefficient j are added, $p \geq 0$, $j > 0$. Then we obtain

the final window function

$$f(x) = j\left(\frac{2}{1.5+\mathrm{sgn}(i)(x-0.5)} - 1\right)^p,$$
$$\mathrm{sgn}(i) = \begin{cases} 1, & i \geq 0, \\ -1, & i < 0. \end{cases} \tag{10}$$

As shown in Fig. 3(a), curves with different p have different trends, i.e., a broad range of adjustment. In Fig. 3(b), the novel window function is used in HP's drift model. It can be seen that terminal overflow and terminal lock are both solved.

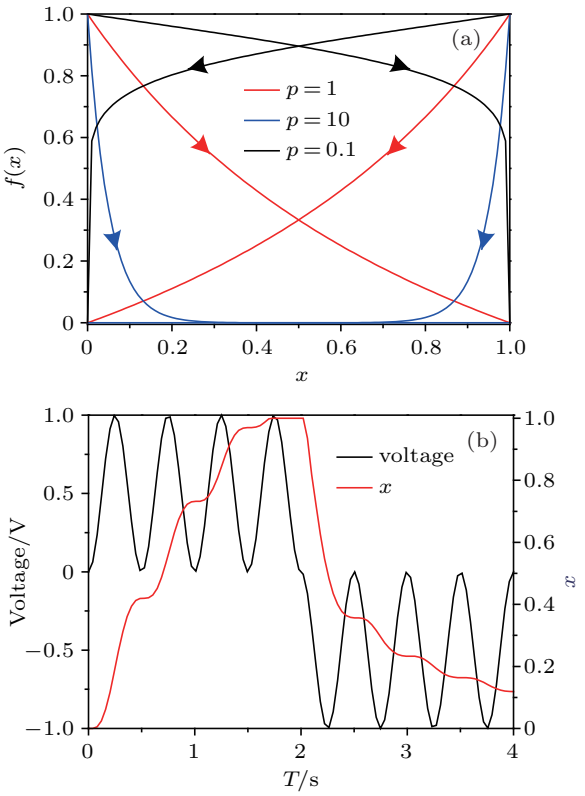


Fig. 3. (color online) (a) The proposed window function and (b) the simulation results in HP's drift model, $j = p = 1$.

In short, our novel window function has obvious advantages compared to the previous ones. It uses two parameters and two variables to overcome all shortcomings, including the terminal overflow and terminal lock. The scale of p is $[0, +\infty)$, which means great flexibility. And j can modify the scale of $f(x)$.

3. Memristor model

3.1. Existing drift diffusion models

Researchers have found the forgetting effect in several memristor experiments. Some models have been proposed to describe this phenomenon. Berdan and Chen proposed different drift diffusion models based on HP's drift model and the research results of Strukov.

Berdan's model is expressed as

$$C_x \frac{\mathrm{d}x}{\mathrm{d}t} = -\frac{x-y}{R_x} + I_0(x), \tag{11}$$

$$C_y \frac{\mathrm{d}y}{\mathrm{d}t} = \begin{cases} I_0(y), & z > q_p \text{ and } v > 0, \\ I_0(y), & z < q_p \text{ and } v < 0, \\ 0, & \text{else}, \end{cases} \tag{12}$$

$$C_z \frac{\mathrm{d}z}{\mathrm{d}t} = i(t) - \frac{z}{R_z}, \tag{13}$$

$$I_0(h) = \frac{\mu_v R_{on} i(t) f(h)}{D^2}. \tag{14}$$

Expression (14) is the same as HP's model, expressions (12) and (13) are added. It is easy to find that y is a reference value for x. z is used to limit the change of y, i.e., y changes its value until z exceeds thresholds. $-(x-y)/R_x$ indicates the effects of mass diffusion and the nucleation process on the drift. By analyzing expression (11), it is easy to find that $\mathrm{d}x/\mathrm{d}t < 0$ when $x = 1$, $i(t) \gg 0$ (also means $I_0(x) = 0$), and $y < 1$. This means that x changes negatively though stimulus is still a great positive one. After a certain negative change ($x < 1$), x changes positively again. There is an oscillation for x, which is not coincident with the memristors. What is more, x no longer changes when $x = y = 1$ and no more stimulus is supplied. This means that the forgetting effect cannot be described. When $x = 0$, there are similar problems. The simulation results are shown in Fig. 4, it can be seen that both x and $\mathrm{d}x/\mathrm{d}t$ have oscillation behaviors, and x can no longer change (or decay) when $x = y = 1$ and no more stimulus is supplied. In brief, Berdan's model has defects when $x = 0, 1$.

Ling Chen's is expressed as

$$\frac{\mathrm{d}x}{\mathrm{d}t} = \left(l - \frac{x-\varepsilon}{\tau}\right) f(x), \quad l = \frac{\mu_v R_{on}}{D^2} i(t), \tag{15}$$

$$\frac{\mathrm{d}\varepsilon}{\mathrm{d}t} = \sigma l f(x), \tag{16}$$

$$\frac{\mathrm{d}\tau}{\mathrm{d}t} = \theta l (a - x). \tag{17}$$

The $-(x-\varepsilon)/\tau$ indicates effects of Fick diffusion and Soret diffusion on the drift. The Fick diffusion has negtive effects and the Soret diffusion has positive effects. Expression (16) expresses the result of Soret diffusion, and expression (17) indicates the decay speed. By analyzing expression (15), it is easy to find that $\mathrm{d}x/\mathrm{d}t$ is limited totally by the window function. As shown in Fig. 5, when $x = 1$, $i(t) \geq 0$, and $f(x) = 0$, x is impossible to change (or decay), even though $l - (x-\varepsilon)/\tau < 0$. When $x = 0$, there is a similar problem. In short, Chen's model also has blemishes when $x = 0, 1$.

3.2. Improved drift diffusion model

Obviously, both Berdan's model and Chen's models have deficiencies when $x = 0, 1$. In this section, an improved drift diffusion model is proposed to overcome problems on terminals ($x = 0, 1$). According to the discussion above, it is easy to find that the limitation of the window function should be decided by $l - (x-\varepsilon)/\tau$ (or $l - (x-y)/R_x$) when $x = 0, 1$. The

improved model can be expressed as

$$\frac{\mathrm{d}x}{\mathrm{d}t} = (l - \omega(x-\varepsilon))k(x), \quad l = \frac{\mu_{\mathrm{v}} R_{\mathrm{on}}}{D^2} i(t), \tag{18}$$

$$k(x) = \begin{cases} \alpha, & \text{if } x = 1 \text{ and } l - \omega(x-\varepsilon) < 0, \\ \alpha, & \text{if } x = 0 \text{ and } l - \omega(x-\varepsilon) > 0, \\ f(x), & \text{otherwise}, \end{cases} \tag{19}$$

$$\frac{\mathrm{d}\varepsilon}{\mathrm{d}t} = \sigma l f(x), \tag{20}$$

where ω is the decay speed, which can be a constant or an expression. In this paper, ω is set as a constant by referencing to Ref. [18]. α and σ are parameters and ε is the final stable value of x. The main difference of the improved model is expression (19). When $x = 1$ and $i(t) \geq 0$, if $l - \omega(x-\varepsilon) < 0$, $\mathrm{d}x/\mathrm{d}t$ is not limited by the window function. When $x = 0$ and $i(t) \leq 0$, if $l - \omega(x-\varepsilon) > 0$, $\mathrm{d}x/\mathrm{d}t$ is not limited by the window function, either. In other cases, $\mathrm{d}x/\mathrm{d}t$ is limited by the window function normally.

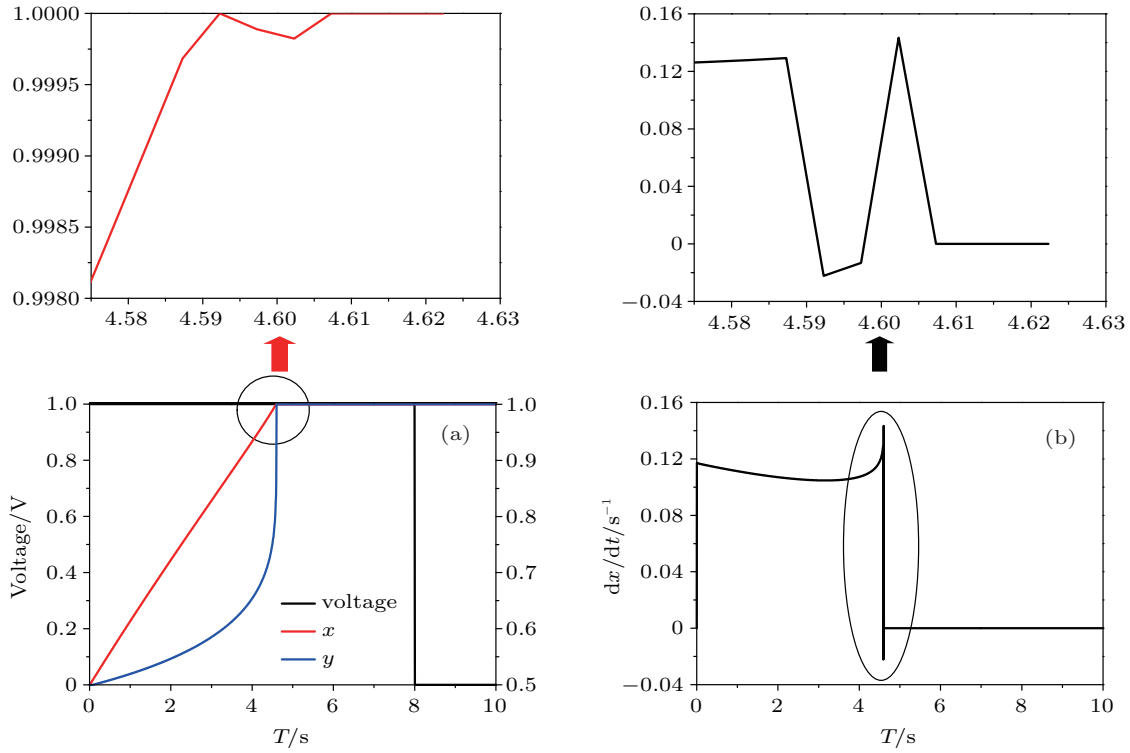


Fig. 4. (color online) (a) Oscillation of x. x remains 1 when $x = y = 1$, $v = 0$. (b) Oscillation of $\mathrm{d}x/\mathrm{d}t$. Parameters are the same as those in Ref. [17].

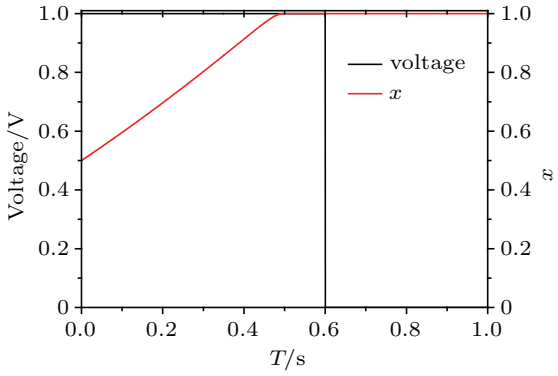


Fig. 5. (color online) x remains 1 when $x = 1$, $i(t) \geq 0$, $f(x) = 0$. The parrameters are the same as those in Ref. [18].

The threshold characteristic has been discovered in several memristors. In order to build a good model, taking the threshold into account is necessary. Expression (18) can turn into

$$l = \frac{\mu_{\mathrm{v}} R_{\mathrm{on}}}{D^2} i(t) g(v), \quad g(v) = \mathrm{stp}(\mathrm{abs}(v) - vt), \tag{21}$$

when l is limited by threshold function $g(v)$. vt is the threshold voltage and $vt > 0$. If the absolute value of stimulus is greater than vt, x changes, otherwise x remains unchanged.

Simulation results of the improved model are shown in Figs. 6 and 7. The window function used in the model is the one proposed in Subssection 2.2. It can be seen that there is an obvious overlap in Figs. 6(a) and 6(c), which means that the improved model can describe the forgetting effects well. Changes of current, resistance, and x with time are shown in Figs. 6(b) and 6(d). In Figs. 7(a) and 7(b), a stimulus of 0.3 V for 50s and 0.01 V for 50 s is applied. When $v = 0.3$ V and $x < 1$, the stimulus is stronger than diffusion, $\mathrm{d}x/\mathrm{d}t > 0$ and x increases. When $v = 0.3$ V and $x = 1$, the stimulus is stronger than diffusion, but $\mathrm{d}x/\mathrm{d}t = 0$ and x remains unchanged. When $v = 0.01$ V, the stimulus is weaker than diffusion, $\mathrm{d}x/\mathrm{d}t < 0$ and x decreases. It is easy to find that x remains unchanged when $|v| < vt$, as shown in Fig. 7(c).

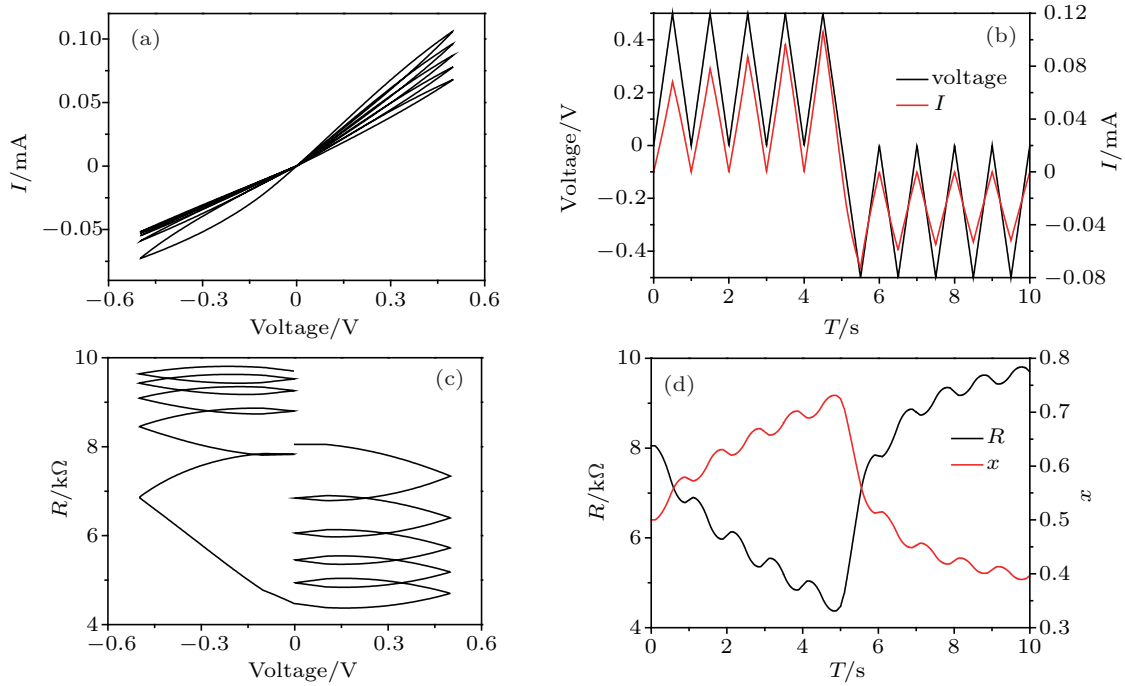


Fig. 6. (color online) Curves of (a) i–v, (b) v–t and i–t, (c) r–v, (d) r–t and x–t of the improved model. Parameters are $\mu_v = 1 \times 10^{-14}$ m/V^2, $D = 10$ nm, $R_{on} = 100\ \Omega$, $R_{off} = 16$ kΩ, $vt = 0.01$ V, $\varepsilon_0 = x_0 = 0.5$, $\omega = 2$, $\sigma = 0.1$, $\alpha = 0.01$, $j = p = 1$.

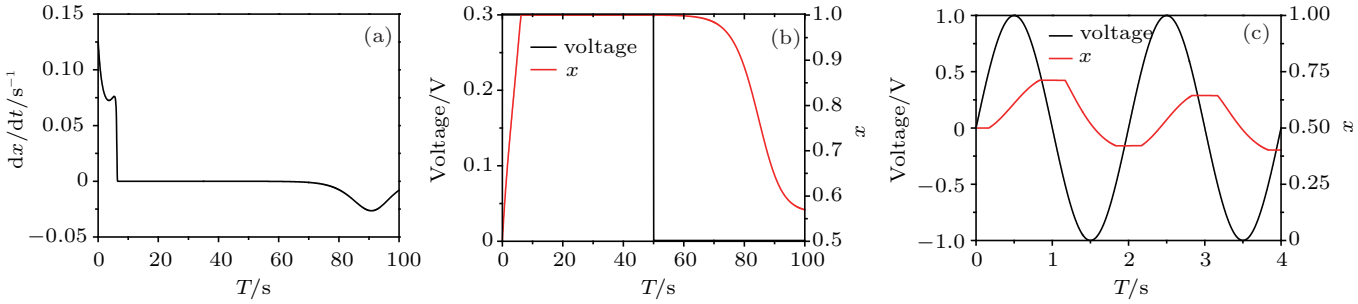


Fig. 7. (color online) Curves of (a) $\mathrm{d}x/\mathrm{d}t$–t and (b) x–t of the improved model. Parameters are the same as those in Fig. 6 and a stimulus of 0.3 V for 50 s and 0.01 V for 50 s is applied. (c) x–t curve, a sine stimulus is applied, $vt = 0.5$ V and the other parameters are the same as those in Fig. 6.

In brief, the improved model overcomes the defects of Berdan's model and Ling Chen's model and can describe the threshold characteristic. So this model can describe the characteristics of memristors better and be used.

3.3. STDP of the improved model

It has been found that memristors have synaptic characteristics and can be used as synapses, this is why memristors are used broadly in brain-inspired computing. Spike-timing-dependent plasticity (STDP) is a significant characteristic of synapses, and is usually used as an evaluation standard of artificial synapses. When a memristor model is used as a synapse model, it is important to have STDP.

As shown in Fig. 8, two spikes, pre-spike and post-spike, are supplied to the improved memristor model. There is a ΔT between achieving time of the two. Simulation results

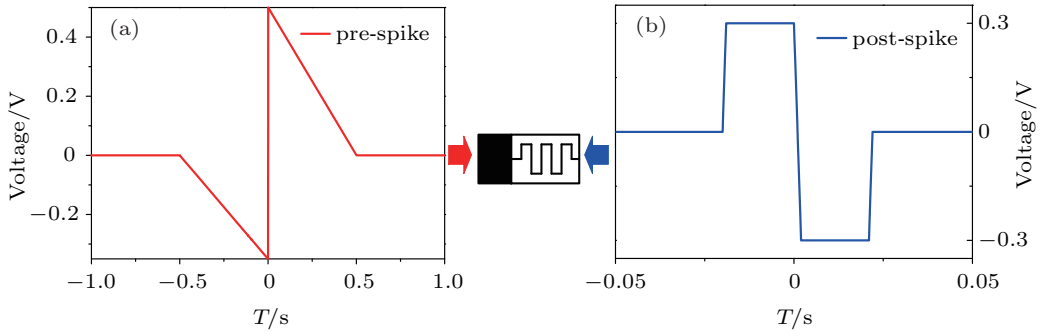


Fig. 8. (color online) (a) Pre-spike and (b) post-spike.

are shown in Fig. 9. It can be seen that the weight change ($\Delta W = \Delta G/G_0 = R_0/R - 1$) of the improved model is dependent on ΔT. What is more, the curve coincides with the standard STDP curve of a biological synapse very well. It means that the improved model can simulate synaptic characteristics well and can be used as a synapse model in brain-inspired computing.

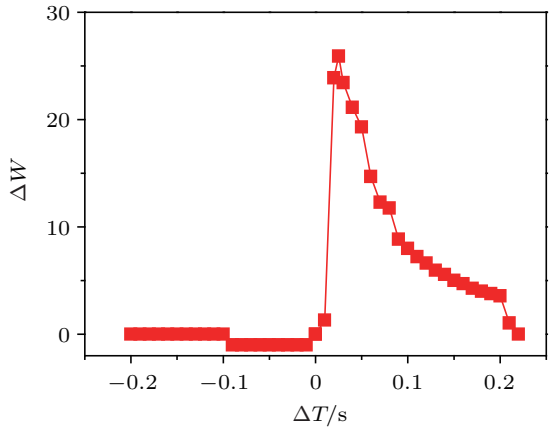


Fig. 9. (color online) Simulation results of STDP learning of the improved model, $vt = 0.6$ V and the other parameters are the same as those in Fig. 6.

4. Application in SNNs

Since memristors can be employed as synapses, composing SNNs with neurons for pattern recognition is an important application of memristors in brain-inspired computing. To demonstrate that the improved model can represent the forgetting effect better in application studies, SNNs based on the improved model, Berdan's model, Chen's model, and the model without forgetting effect respectively are employed to recognize digit images of "0"–"9". As shown in Fig. 10(a), there are 15 input neurons (pre_0–pre_14) and 10 output neurons (post_0–post_9) in the SNNs. Additionally, there is a memristor between each pair of input neurons and output neurons. Digit images of "0"–"9" are composed by 15 blocks, which are depicted in Fig. 10(b). The neuron is a kind of integrate-and-fire, which integrates charges from pre-synapses and generates a voltage spike when the voltage corresponding to the integrated charges exceeds a threshold voltage.

Before training, the states of all memristors are mid-resistance, which means that the models are set as $x_0 = 0.5$. During the training process, the memristors corresponding to the black blocks are trained to LRS and the memristors corresponding to the white blocks are trained to HRS, which means that all memristors are in the terminal state. The states of the memristors after training are shown in Fig. 11(a). During the recognizing process, when a digit image is supplied as the input, the input neurons corresponding to the black blocks generate a square pulse and send it to the output neurons via memristors, the input neurons corresponding to the white blocks generate nothing. Then, the integrated voltage of post_0–post_9 changes with time, and recognition is finished when there is a post neuron exceeding the threshold voltage.

Recognizing image "1" from other images is shown as an example. As shown in Fig. 11(b), post_1 exceeds the threshold voltage first with the memristors after training. After 80 s, the states of the memristors described by the improved model are shown in Fig. 11(c), which indicates that the resistance of the memristors changes due to the forgetting effect. As shown in Fig. 11(d), the voltage changes more smoothly and the maximum voltage that post_1 can reach is lower than that in Fig. 11(b). However, when Berdan's model, Chen's model, and the model without forgetting effect are employed in the SNNs, the states of the memristors and the integrated voltages of the output neurons have no difference compared to those in Fig. 11(b), which means that the forgetting effect is not present at all. The recognition of other digit images gets similar results.

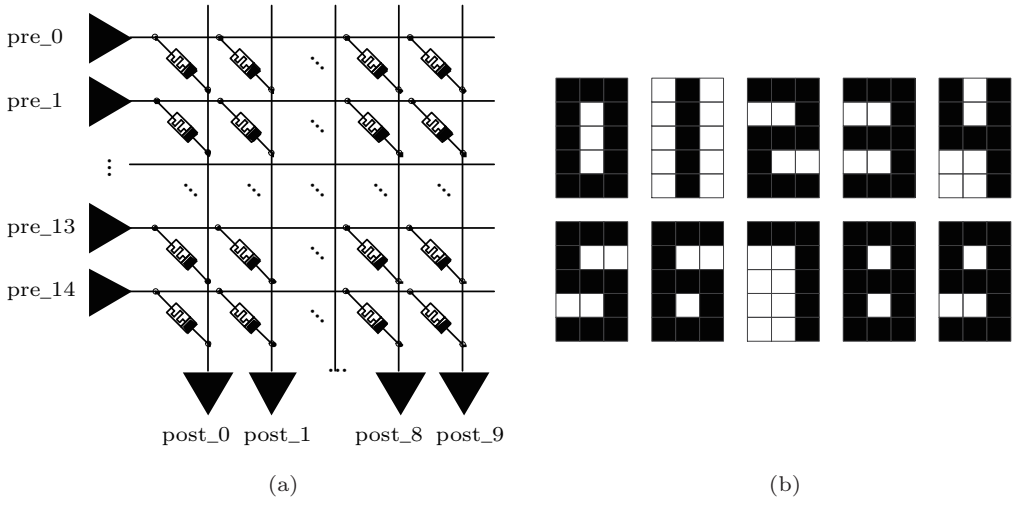


Fig. 10. (a) SNNs based on memristors and neurons, and (b) digit images of "0"–"9".

When the forgetting effect can influence memristors' states, taking the forgetting effect into account is essential when the memristor model is employed as the synapse in the studies of brain-inspired computing. From the simulation results, we can find that the improved model can express the forgetting effect of memristors better than the other models. The results also indicate that there will be an inaccurate evaluation of recognition if the other models are used to simulate the forgetting effect, but a more appropriate evaluation can be obtained when the improved model is used. Therefore, the improved model can work better in the situations that the forgetting effect plays a significant role.

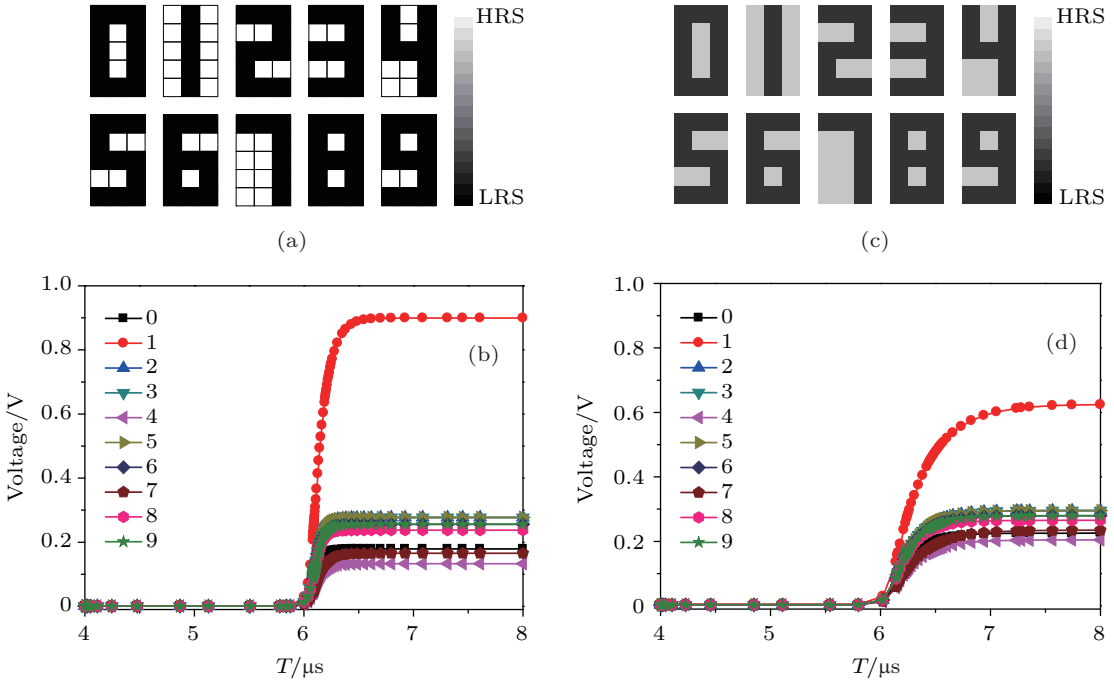


Fig. 11. (color online) (a) States of memristors with different models after training, (b) results of recognizing image "1" with states of memristors in (a), (c) states of memristors with the improved model after forgetting, and (d) results of recognizing image "1" with states of memristors in (c).

5. Conclusion

A novel window function is proposed and has good performance. Deficiencies on $x = 0$, 1 of the previous drift diffusion models are analyzed, and an improved drift diffusion model is presented. The improved model deals well with influences of diffusion on drift when $x = 0$, 1. The threshold characteristic is added to the improved model to make it more common and the STDP curve of the improved model coincides with the biological synapse well. Different models are used as synapses respectively in SNNs to recognize digit images to examine their performances in representing the forgetting effect. Simulation results show that the improved model can express the forgetting effect better than the previous models.

References

[1] Chua L O 1971 *IEEE Tran. Circ. Th.* **18** 507
[2] Strukov D B, Snider G S, Stewart D R and Williams R S 2008 *Nature* **453** 80
[3] Zhou J, Yang X J, Wu J J, Zhu X, Fang X D and Huang D 2013 *Sci. China: Inf. Sci.* **56** 1
[4] Zhu X, Tang Y H, Wu C Q, Wu J J and Yi X 2014 *Chin. Phys. B* **23** 028501
[5] Su S, Jian X C, Wang F, Han Y M, Tian Y X, Wang X Y, Zhang H Z and Zhang K L 2016 *Chin. Phys. B* **25** 107302
[6] Li Z J and Zheng Y C 2013 *Chin. Phys. B* **22** 040502
[7] Huang D, Wu J J and Tang Y H 2014 *Chin. Phys. B* **23** 038404
[8] Jo S H, Chang T Ebong I, Bhadviya B B, Mazumder P and Lu W 2010 *Nano Lett.* **10** 1297
[9] Covi E, Brivio S, Serb A, Prodromakis T, Fanciulli M and Spiga S 2016 *Front. Neurosci.* **10** 482
[10] Zhang Y, Li Y, Wang X P and Friedman E G 2017 *IEEE Tran. Elec. Dev.* **64** 1806
[11] Joglekar Y N and Wolf S J 2009 *Eur. J. Phys.* **30** 661
[12] Biolek Z, Biolek D and Biolkova V 2009 *Radioengineering* **18** 210
[13] Prodromakis T, Peh B P, Papavassiliou C and Toumazou C 2011 *IEEE Tran. Elec. Dev.* **58** 3099
[14] Zha J X, Huang H and Liu Y J 2016 *IEEE Tran. Circuits Syst. II: Exp. Briefs* **63** 423
[15] Chang T, Jo S H, Kim K H, Sheridan P, Gaba S and Lu W 2011 *Appl. Phys. A* **102** 857
[16] Chang T, Jo S H and Lu W 2011 *ACS Nano* **5** 7669
[17] Wang Z Q, Xu H Y, Li X H, Yu H, Liu Y C and Zhu X J 2012 *Adv. Funct. Mater.* **22** 2759
[18] Meng F Y, Duan S K, Wang L D, Hu X F and Dong Z K 2015 *Acta Phys. Sin.* **64** 148501 (in Chinese)
[19] Shao N, Zhang S B and Shao S Y 2016 *Acta Phys. Sin.* **65** 128503 (in Chinese)
[20] Strukov D B, Alibart F and Wiliams R S 2012 *Appl. Phys. A* **107** 509
[21] Berdan R, Lim C, Khiat A and Papavassiliou C 2014 *IEEE Elec. Dev. Lett.* **35** 135
[22] Chen L, Li C D, Huang T W, Ahmad H G and Chen Y R 2014 *Phys. Lett. A* **378** 2924